# Electron-lattice coupling in congruent Co-doped $LiNbO_3$:$Cr^{3+}$:ZnO crystal



2001 J. Phys.: Condens. Matter 13 6577

(http://iopscience.iop.org/0953-8984/13/30/313)

INSTITUTE OF PHYSICS PUBLISHING JOURNAL OF PHYSICS: CONDENSED MATTER

J. Phys.: Condens. Matter **13** (2001) 6577–6583 PII: S0953-8984(01)22081-5

# Electron–lattice coupling in congruent Co-doped $LiNbO_3$:$Cr^{3+}$:ZnO crystal

**G A Torchia**[1,2,3], **O Martinez Matos**[1], **P Vaveliuk**[1,2] **and J O Tocho**[1,2]

[1] Centro de Investigaciones Opticas CIC—CONICET, Argentina
[2] Departamento de Física, Facultad de Ciencias Exactas, Universidad Nacional de La Plata, Argentina

E-mail: gustavot@ciop.unlp.edu.ar (G A Torchia)

Received 19 February 2001
Published 13 July 2001
Online at stacks.iop.org/JPhysCM/13/6577

**Abstract**

The importance of the role of the ion–lattice coupling in determining the energy levels of $Cr^{3+}$ ions in congruent $LiNbO_3$ crystals doped with 2.9% of ZnO is demonstrated in this paper. The Racah parameters: $B = 533\ cm^{-1}$, $C = 3244\ cm^{-1}$ and the crystal-field intensity $Dq = 1527\ cm^{-1}$ were determined and the Tanabe–Sugano diagram was constructed. The characteristics of the absorption and the emission spectra of $Cr^{3+}$ ions in these crystals can be explained in terms of the configurational-coordinate diagram in the harmonic approximation, with good agreement obtained. The Huang–Rhys parameter $S = 6.86$ and the lattice phonon energy $\hbar\omega = 343\ cm^{-1}$ are also reported in this work.

## 1. Introduction

In the last few years there has been great interest in developing lithium niobate crystals doped with transition metals and rare-earth ions for use in laser and non-linear optics devices. The strong photorefractive effect that lithium niobate presents is a severe drawback as regards laser applications but can be quenched by adding around 5% of MgO or ZnO to the melt. Several examples of high-efficiency lasers based on doubly doped lithium niobate have been reported [1–3].

The $Cr^{3+}$ ion is a good candidate for doping lithium niobate in order to obtain broad-spectrum tunable lasers [4]. It was suggested that $Cr^{3+}$ substitutes for $Li^{+}$ in singly doped crystal and it has been proved that most of the chromium ions are found approximately at the $Nb^{5+}$ positions in crystals heavily co-doped with $Mg^{2+}$ or $Zn^{2+}$ [5–10]. Another substitution mechanism has been proposed in which two chromium ions substitute simultaneously for a pair

[3] Author to whom any correspondence should be addressed. Gustavo Adrián Torchia, Centro de Investigaciones Opticas, CC 124, 1900 La Plata (BsAs), Argentina; telephone: (54-221) 484-0280; fax: (54-221) 471-2771.

  

of $Li^+$ and $Nb^{5+}$ ions to compensate the charge [11]. At both sites the $Cr^{3+}$ experiences a nearly octahedral electric field produced by two planes of $O^{2-}$ ligands. The influence of the crystal field on transition metal ions is very strong because the extended $3d^n$ electron configuration is substantially affected by this field. The energy levels for different $d^n$ electron configurations in a rigid environment with one octahedrally coordinated lattice have been calculated by Tanabe and Sugano [12]. The energy values have been tabulated in terms of the Racah parameters $A$, $B$ and $C$ and the crystal field $Dq$. For a $3d^3$ system like chromium in lithium niobate, the energy that results from the Coulomb interaction between the electrons and the interaction between the electrons and the octahedral crystal field are given in table 1. There is a single $^4A_2$ ground state with energy $-15B$ that does not depend on the crystal field; similarly there are only single $^4T_2$, $^2A_1$ and $^2A_2$ states. There are two $^4T_1$ states whose energies can be obtained by diagonalization of the $2 \times 2$ matrix shown in the table. Similarly the energy of the $^2E$, $^2T_1$ and $^2T_2$ states can be calculated from a matrix also shown in table 1. The lowest-energy $^2E$ state is important because it is the lowest-energy excited state of many chromium systems that show sharp luminescence (R lines).

**Table 1.** Matrix elements of the crystal-field and Coulomb interactions and energy levels for the relevant $d^3$ states in octahedral symmetry, from reference [13].

$$E(^4T_1) = \begin{pmatrix} 10Dq - 3B & 6B \\ 6B & 20Dq - 12B \end{pmatrix}$$

$$E(^2T_2) = \begin{pmatrix} 5C & -3\sqrt{3}B & -5\sqrt{3}B & 4B + 2C & 2B \\ -3\sqrt{3}B & 10Dq - 6B + 3C & 3B & -3\sqrt{3}B & -3\sqrt{3}B \\ -5\sqrt{3}B & 3B & 10Dq + 4B + 3C & -3\sqrt{3}B & \sqrt{3}B \\ 4B + 2C & -3\sqrt{3}B & -3\sqrt{3}B & 20Dq + 6B + 5C & 10B \\ 2B & -3\sqrt{3}B & \sqrt{3}B & 10B & 20Dq - 2B + 3C \end{pmatrix}$$

$$E(^2T_1) = \begin{pmatrix} -6B + 3C & -3B & 3B & 0 & -2\sqrt{3}B \\ -3B & 10Dq + 3C & -3B & 3B & 3\sqrt{3}B \\ 3B & -3B & 10Dq - 6B + 3C & -3B & -\sqrt{3}B \\ 0 & 3B & -3B & 20Dq - 6B + 3C & 2\sqrt{3}B \\ -2\sqrt{3}B & 3\sqrt{3}B & -\sqrt{3}B & 2\sqrt{3}B & 20Dq - 2B + 3C \end{pmatrix}$$

$$E(^2E) = \begin{pmatrix} -6B + 3C & -6\sqrt{2B} & -3\sqrt{2B} & 0 \\ -6\sqrt{2B} & 10Dq + 8B + 6C & 10B & \sqrt{3}(2B + C) \\ -3\sqrt{2B} & 10B & 10Dq - B + 3C & 2\sqrt{3}B \\ 0 & \sqrt{3}(2B + C) & 2\sqrt{3}B & 30Dq - 8B + 4C \end{pmatrix}$$

$$E(^4T_2) = 10Dq - 15B$$

$$E(^2A_1) = 10Dq - 11B + 3C$$

$$E(^2A_2) = 10Dq + 9B + 3C$$

$$E(^4A_2) = -15B$$

Purely electronic transitions in perfect crystals have linewidths determined entirely by the lifetime and dephasing mechanisms. The interaction between optically active impurity ions and the vibration of the host lattice is of great importance for understanding optical transitions in real crystals. In this paper we present the absorption and emission characteristics of $Cr^{3+}$ in congruent lithium niobate co-doped with ZnO. The ion–lattice coupling is analysed in terms of the configurational-coordinate breathing model in the harmonic approximation. The Huang–Rhys parameter $S$ and the phonon energy are determined on the basis of this model.

## 2. Experimental procedure

The samples used in this work were grown by the Czochralski method in the open air, starting with amounts of $Li_2O$ and $Nb_2O_5$ that ensure congruent concentrations in the crystal. The doping concentrations in the melt were 3% for ZnO and 0.15% for $Cr_2O_3$. The composition of the crystals was analysed by means of the EXTF (fluorescence total x-ray emission); the results for chromium and zinc ions were 0.1% and 2.9% respectively, normalized to the $Nb^{5+}$ concentration. Congruent crystals have a composition of $Li_{0.945}Nb_{1.05}O_3$ instead of the stoichiometric composition $LiNbO_3$. The samples was cut in slices of 1 mm width, reduced to dice of dimensions $1 \times 4 \times 6$ mm and polished with diamond powders of different diameters.

The optical absorption spectrum was taken at room temperature with a commercial spectrophotometer (Hitachi U-3501). The continuous-wavelength (cw) emission spectrum was taken at room temperature using an argon multiline laser as the excitation source and detecting the light with an AsGaIn (Hamamatsu 751 K) cooled photomultiplier. The luminescence was dispersed by a 0.5 m monochromator (SPEX 5000M) and amplified by a lock-in (EE&G). The absorption and emission spectra were analysed with a multi-Gaussian fitting and the energy levels reported below correspond to peak values of the fitting.

## 3. Results and discussion

Figure 1 presents the absorption and emission spectra at room temperature for congruent lithium niobate crystals co-doped with $Cr^{3+}$ and ZnO (2.9%). The absorption spectrum shows two broad bands centred at 20 770 $cm^{-1}$ (481 nm) and 15 274 $cm^{-1}$ (655 nm) associated with vibronic transitions of the $Cr^{3+}$. The band centred at 481 nm is associated with the $^4A_2 \rightarrow {}^4T_1$ transition while the band centred at 660 nm is associated with the $^4A_2 \rightarrow {}^4T_2$ transition; both bands are spin allowed. In this spectrum there are also present three weak peaks centred at 19 607 $cm^{-1}$ (510 nm), 14 705 $cm^{-1}$ (680 nm) and 13 755 $cm^{-1}$ (727 nm) corresponding to the spin-forbidden transitions $^4A_2 \rightarrow {}^2T_2$, $^4A_2 \rightarrow {}^2T_1$ and $^4A_2 \rightarrow {}^2E$ [11]. As can be seen in figure 1, the emission spectrum has a broad band centred at 10 883 $cm^{-1}$ (919 nm); this band was assigned previously to the transition $^4T_2 \rightarrow {}^4A_2$ that corresponds to $Cr^{3+}$ ions at $Li^+$ sites of congruent lithium niobate crystals because the content of Zn is not sufficient to induce the occupation of the Nb site [6].

From the energy level values obtained, the strength of the octahedral crystal field $Dq$ and the spectroscopic Racah parameters $B$ and $C$ are calculated. The magnitude of $Dq$ is obtained directly from the energy corresponding to the peak of the $^4A_2 \rightarrow {}^4T_2$ absorption band, which is $10Dq$:

$$Dq = [E(^4T_2) - E(^4A_2)]/10 = 1527\ \text{cm}^{-1}. \tag{1}$$

If we write $\Delta E$ for the energy difference between the $^4T_2$ and the lowest $^4T_1$ state, which experimentally is the separation between the two strong absorption bands in figure 1, the $B$-value can be obtained from

$$\frac{B}{Dq} = \left[\left(\frac{\Delta E}{Dq}\right)^2 - 10\left(\frac{\Delta E}{Dq}\right)\right] \Big/ 15\left(\frac{\Delta E}{Dq} - 8\right). \tag{2}$$

For $Dq = 1527\ \text{cm}^{-1}$ and $\Delta E = 5496\ \text{cm}^{-1}$, the result $B = 533\ \text{cm}^{-1}$ is obtained.

The last Racah parameter can be calculated from an approximate expression given by Henderson and Imbusch [14]:

$$C = [E(^2E) - 7.9B + 1.8B^2/Dq]/3.05. \tag{3}$$

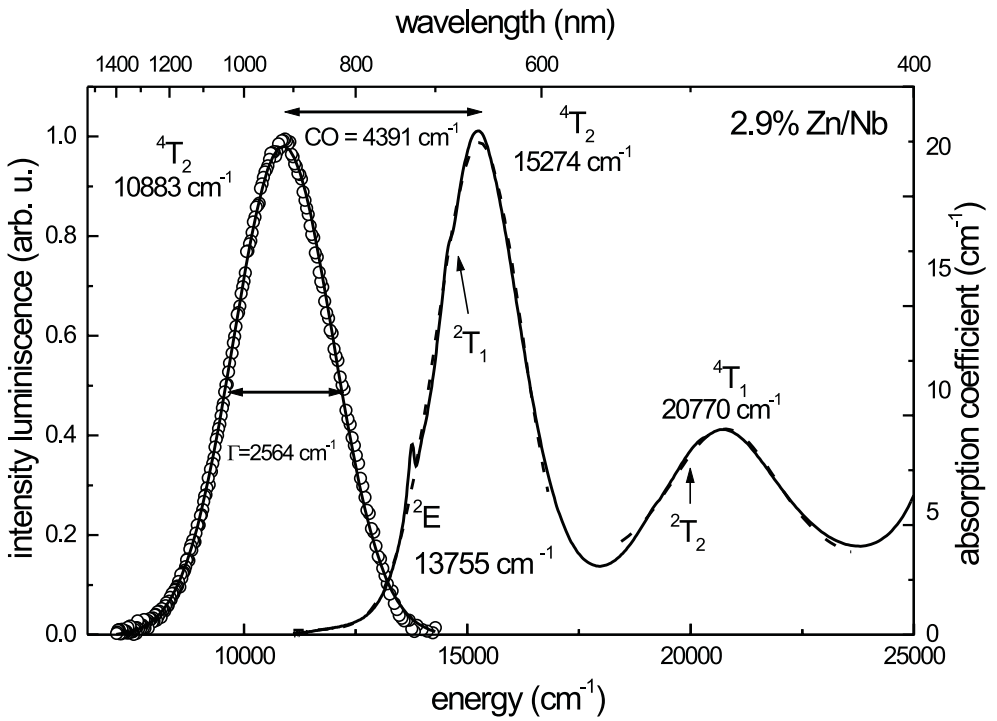


**Figure 1.** Room temperature absorption and luminescence spectra of $Cr^{3+}$ ions in $LiNbO_3$ (2.9% of ZnO) crystal. The energy values of relevant levels, the Stokes shift ($CO$) and the FWHM bandwidth ($\Gamma$) of the emission band are indicated.

Using the experimental value $E(^2\mathrm{E}) = 13\,755\ \mathrm{cm}^{-1}$ and the values found previously for $Dq$ and $B$, the result $C = 3238\ \mathrm{cm}^{-1}$ is obtained. More accurate determination of $C$ requires the diagonalization of the $4 \times 4$ matrix corresponding to the $^2$E states given in table 1. The lowest eigenvalue gives the analytical expression necessary to calculate $C = 3244\ \mathrm{cm}^{-1}$ by solving a transcendental equation.

With the Racah parameters found above, the Tanabe–Sugano diagram for the $Cr^{3+}$ ions was constructed. The energy for the most relevant states, taking the energy of the $^4A_2$ state equal to zero, can be calculated by using equations (1)–(3):

$$\begin{aligned} E(^4\mathrm{A}_2)/B &= 0 \\ E(^4\mathrm{T}_2)/B &= 10/a \\ E(^4\mathrm{T}_1)/B &= \{20 + 15a - [(10 + 15a)^2 - 480a]^{1/2}\}/2a \\ E(^2\mathrm{E})/B &= 3.05C/B + 7.90 - 1.80a \end{aligned} \tag{4}$$

where $a = B/Dq$.

The Tanabe–Sugano diagram constructed in this manner for the main spectroscopic states of $Cr^{3+}$ in congruent lithium niobate is presented in figure 2. The vertical broken line represents the appropriate value for $Dq/B$ (2.86) found for this crystal. The diagram presents one important contradiction: the lower-energy excited level in the Tanabe–Sugano representation is the state $^2$E while the broad band of luminescence observed experimentally indicates that the lower level must be the $^4T_2$ state. The energy of the $^2$E state shows little dependence on the crystal field, similarly to that of the ground state $^4A_2$, so the emission between these levels

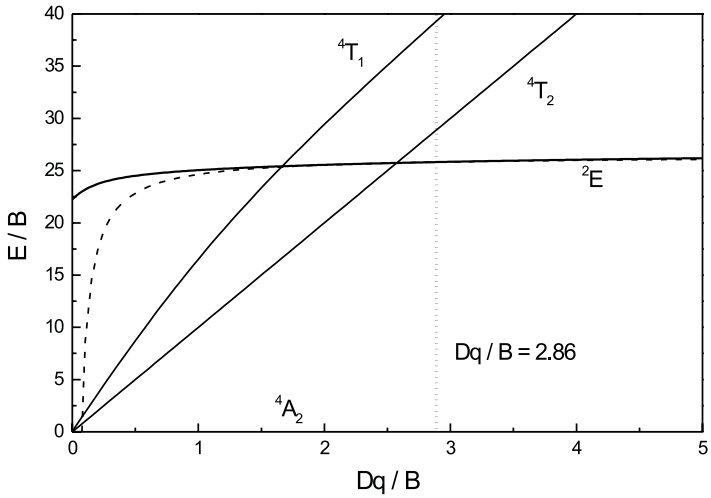


**Figure 2.** The Tanabe–Sugano diagram for $Cr^{3+}$ in $LiNbO_3$:ZnO (2.9%) crystal corresponding to the experimental values obtained in this work. The solid line for the $^2E$ level corresponds to the exact diagonalization of the matrix in table 1 while the dashed line is the approximation given by equation (3).

gives a narrow band (R line). The $^4T_2$ state with its greater dependence on the crystal field can give rise to a broad band of luminescence.

Big errors in the crystal-field determination that displace the position of the value of $Dq/B$ enough to invert the positioning of the $^4T_2$ and $^2E$ energies must be excluded because the absorption spectra are consistent with the diagram of figure 2. To explain the contradiction, the octahedral vibration and the electron–lattice coupling must be considered. As a first approximation, the vibrating environment can be modelled by the single-configurational-coordinate model in the harmonic approximation.

The configurational-coordinate model assumes that the distance $Q$ from the active ion to its first shell of neighbouring ions pulsates harmonically about its equilibrium value $Q_0$. The vibration energy can be written as $m\hbar\omega$, where $m$ is the number of vibrating quanta and $\omega$ is the breathing frequency. As a further approximation, the same breathing frequency is considered for all of the electronic states. The equilibrium values for $Q$ are specific to each electronic state. The departure from the average of $Q$ corresponds to the difference in coupling between the ion and the lattice. The larger the coupling, the larger the difference between equilibrium values. As usual, the difference in electron–lattice coupling is characterized by a dimensionless constant, the Huang–Rhys parameter, $S$, defined as the number of vibrating quanta excited in the most probable absorption transition.

For the determination of the phonon energy and the Huang–Rhys parameter we used the spectroscopic data of figure 1. The absorption and emission bands from transitions that connect the $^4A_2$ and $^4T_2$ states are approximately Gaussians and mirror images of each other; for this case the Stokes shift, the difference in energy between the absorption and emission band peaks, can be related to $S$ by

$$CO = (2S - 1)\hbar\omega \tag{5}$$

where $CO$ is the Stokes shift. Another equation necessary to calculate the phonon energy and the Huang–Rhys parameter is given by the expression for the bandwidth, which at room

temperature can be written as

$$\Gamma(T) = 2.35\hbar\omega(S\coth(\hbar\omega/kT))^{1/2} \tag{6}$$

where $\Gamma(T)$ stands for the FWHM of the emission band; $k = 0.695\ \mathrm{cm}^{-1}\ \mathrm{K}^{-1}$ is Boltzmann's constant. Using equations (5) and (6) and the values found experimentally for the Stokes shift and the bandwidth ($CO = 4391\ \mathrm{cm}^{-1}$, $\Gamma(T) = 2564\ \mathrm{cm}^{-1}$), we get $\hbar\omega = 343\ \mathrm{cm}^{-1}$ and $S = 6.86$ for $T = 295$ K.

The energy level scheme of $Cr^{3+}$ in congruent lithium niobate crystals is presented in figure 3. The new level diagram shows that the electron–lattice coupling is sufficiently large to explain why the minimum electronic energy of the $^4T_2$ manifold is below the energy of the $^2E$ state.

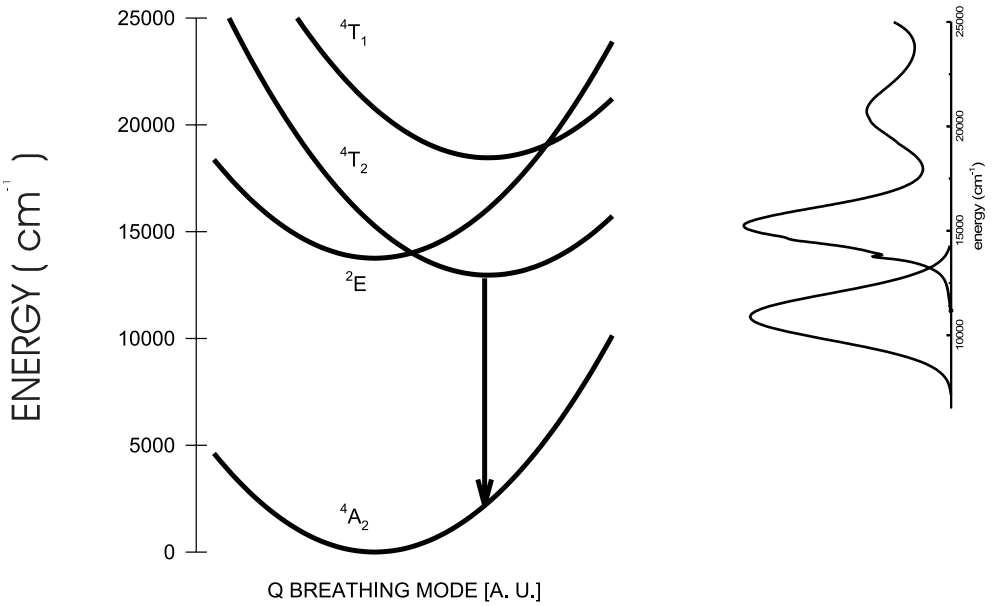


**Figure 3.** The configurational-coordinate diagram for $Cr^{3+}$ in $LiNbO_3$:ZnO (2.9%) crystal.

## 4. Conclusions

In this paper we have presented the crystal-field strength, the spectroscopic Racah parameters, the Huang–Rhys parameter and the breathing-mode phonon frequency corresponding to the $Cr^{3+}$ ion in congruent lithium niobate crystal co-doped with 2.9% of ZnO. The crystal-field strength $Dq$ and Racah parameters are found; the values are similar to ones reported previously for other lithium niobate samples [15, 16]; the Huang–Rhys parameter obtained, $S = 6.86$, is identical to that estimated by Weiyi Jia *et al* [11] for a sample of $Cr^{3+}$:$LiNbO_3$ without specification of the congruency. The breathing phonon energy was determined to our knowledge for the first time for congruent lithium niobate co-doped with $Cr^{3+}$ and $Zn^{2+}$. This medium-hard phonon (343 $\mathrm{cm}^{-1}$) can be coupled with the $TO_3$ phonon of the bulk lithium niobate, which was found from Raman measurements at 332 $\mathrm{cm}^{-1}$ for a nearly stoichiometric sample at room temperature [17]. Similarly, Ridah *et al* [18] working with congruent samples have found LO phonons at 345 $\mathrm{cm}^{-1}$ and TO phonons at 322 and 369 $\mathrm{cm}^{-1}$. Because the

breathing mode at 343 $cm^{-1}$ can be strongly coupled to the bulk phonons, the non-radiative process can compete with the radiative process even for energy gaps over 10 000 $cm^{-1}$; consequently the fluorescence quantum yield could be low in these crystals. Recently the fluorescence quantum yield of $Cr^{3+}$ at lithium sites in congruent lithium niobate co-doped with ZnO was found to range around 5% [19].

## References


[1] Volk T R, Rubinina N M and Wöhlecke V I M 1994 *J. Opt. Soc. Am.* B **11** 1681–7
[2] Jaque D, Capmany J, García-Solé J, Brenier A and Boulon G 2000 *Appl. Phys.* B **70** 11–14
[3] Montoya E, Capmany J, Bausá L E, Kellner T, Diening A and Haber G 1999 *Appl. Phys. Lett.* **74** 3113–15
[4] Qiu Y 1993 *J. Phys.: Condens. Matter* **5** 2041–4
[5] Diaz-Caro J, García-Solé J, Bravo D, Sanz-García J A, López F J and Jaque F 1996 *Phys. Rev.* B **54** 13 042–6
[6] Torchia G A, Sanz-García J A, Díaz-Caro J, Han T and Jaque F 1998 *Chem. Phys. Lett.* **288** 65–70
[7] Torchia G A, Sanz-García J A, López F J, Bravo D, García-Solé J, Jaque F, Gallagher H G and Han T P J 1998 *J. Phys.: Condens. Matter* **10** L341–5
[8] Corradi G, Soethe H, Spaeth J M and Polgár K 1991 *J. Phys.: Condens. Matter* **3** 1901–8
[9] Martín A, López F J and Agulló-López F 1992 *J. Phys.: Condens. Matter* **4** 847–53
[10] Kling A, Soares J C, da Silva M F, Sanz-García J A, Dieguez E and Agulló-López F 1998 *Nucl. Instrum. Methods Phys. Res.* B **136–138** 426–30
[11] Jia W, Liu H, Knutson R and Yen W M 1990 *Phys. Rev.* B **41** 10 906–10
[12] Tanabe Y and Sugano S 1954 *J. Phys. Soc. Japan* **9** 753–66
[13] Sugano S J, Tanabe Y and Kamikura H 1970 *Multiplets of Transition Metal Ions in Crystals* (New York: Academic)
[14] Henderson B and Imbush G F 1989 *Optical Spectroscopy of Inorganic Solids* (Oxford: Oxford Science)
[15] Macfarlane P I, Holliday K, Nicholls J F H and Henderson B 1995 *J. Phys.: Condens. Matter* **7** 9643–56
[16] Camarillo E, Tocho J O, Vergara I, Dieguéz E, García-Solé J and Jaque F 1990 *Phys. Rev.* B **45** 4600–4
[17] Ridah A, Fontana M D and Bourson P 1997 *Phys. Rev.* B **56** 5967–73
[18] Ridah A, Bourson P, Fontana M D and Malovichko G 1997 *J. Phys.: Condens. Matter* **9** 9687–93
[19] Torchia G A, Muñoz J A, Cusso F, Jaque F and Tocho J O 2001 *J. Lumin.* **92** 317–22